$\mathcal{L}_1$ ADAPTIVE SPEED CONTROL FOR A HELICOPTER

Giulia Bertolani, giulia.bertolani2@unibo.it, University of Bologna, (Italy)
Andrea D. Ryals, andrea.ryals@phd.unipi.it, University of Pisa, (Italy)
Lorenzo Pollini, lorenzo.pollini@unipi.it, University of Pisa, (Italy)
Fabrizio Giulietti, fabrizio.giulietti@unibo.it, University of Bologna, (Italy)

Abstract

Adaptive control theory is used to improve robustness of systems against model uncertainties and disturbances. Two of the main drawbacks of adaptive controllers is the lack of criteria to measure the robustness of the controller and the speed of the adaptation loop. In $\mathcal{L}_1$ adaptive control theory both problems are solved by the introduction of a low pass filter in the control input. The $\mathcal{L}_1$ adaptive control robustness and stability are guaranteed by numerical criteria. $\mathcal{L}_1$ adaptive control raised a great interest in the aerospace field due to the presence of nonlinear and uncertain dynamics that affects aircraft flight performances. Such strategy by the way has not been widely used and explored for rotorcrafts. In this article the authors propose an $\mathcal{L}_1$ output feedback speed controller for helicopters. The control system architecture is tested by means of a simulation test campaign through the use of a nonlinear helicopter model. Both performances and robustness of the controller are evaluated, even in presence of disturbances.

1. INTRODUCTION

The use of unmanned small-scale helicopters has been increasing along the last decade because of their capability to operate in a wide range of flight conditions performing different tasks, such as load transportation, surveillance, search and rescue, agricultural and remote sensing applications, etc.,[1].[2] Indeed, the main advantages in the use of rotary-wing aircraft are the capability of these vehicles to perform hovering and vertical climb/descent.[3] With respect to full-scale helicopters, small-scale platforms show the same flight characteristics and similar dynamics;[4] this makes such vehicles as perfect benchmarks for advanced control strategies that may be used on larger scale aircraft in the near future. Moreover, the small scale platforms have reduced costs that allows these vehicles to be used in experimental contexts. However, helicopters are inherently unstable with significant dynamic coupling and a huge workload is required to the pilot.

Proportional-Integral-Derivative (PID) controllers are widely used for their simplicity and show satisfactory performance in a lot of applications.[5] At the same time, due to the high complexity of the helicopters and their operating flight conditions, PID controllers are not able to provide the desired flying qualities to complete all the tasks. The PID design do not manage to suppress the coupling effects between longitudinal and lateral axes.[4] Adaptive control gives a suitable solution to overcome these problems.[6] The adaptive contribution is required to be enough robust and fast. The $\mathcal{L}_1$ adaptive control is chosen for its capability to decouple robustness from fast adaptation.[7] The control theory is introduced by Hovakimyan and Cao in references,[8],[9].[10] With special regard to the aerospace sector, there are many successful applications. Considering fixed-wing aircraft, Gregory et al.[11] developed an $\mathcal{L}_1$ control system taking care of both matched and unmatched uncertainties. The controller has been tested in case of failures and in areas of the flight envelope that present highly non-linearity. Wang et al.[12] made use of the $\mathcal{L}_1$ adaptive control with neural network based predictor for autonomous aerial refuelling. Hellmundt et al.[13] the $\mathcal{L}_1$ adaptive control has been used to deal with uncertainties on a fighter aircraft leading to an improvement in system performance. In the field of rotary wing aircraft, Bichlmeier et al.[14] and Song et al.[15] presented a piecewise constant adaptation law respectively on attitude rate control loop and for helicopter vertical flight. Guerriero et al.[16] developed a state space stabilization of speed for an autonomous small-scale helicopter along with $\mathcal{L}_1$ adaptive controller augmentation. Finally, in a recent work of the same authors,[17] an $\mathcal{L}_1$ adaptive control system has been developed to improve performances and robustness of a PID attitude controller of an unmanned small-scale helicopter.

In the present research paper an $\mathcal{L}_1$ adaptive speed control system capable of keeping the desired nominal performances in a broad range of flight conditions and in presence of wind disturbances is proposed. The main contribution of this paper is the development of an

adaptive $\mathcal{L}_1$ output feedback controller for a helicopter. The design of this controller is based over the identified attitude dynamics of the system controlled trough PID attitude controllers. This choice allows to simplify the adaptive control design. As a matter of fact, in such a way $\mathcal{L}_1$ has to deal with a yet stable attitude dynamic. This approach is novel in the field of helicopter control. The selected adaptive controller architecture and the results of a simulation campaign are given. The robustness and tracking performance of the control system are discussed. In addition, the pilot workload reduction is proved in a simulation test in which the same pilot commands are given to the system both in presence and in absence of disturbances. The control laws have been tested on a nonlinear model of a small-scale remotely piloted helicopter. Simulations are carried out in Matlab/Simulink® environment, that is used to implement the vehicle model and control laws.

The paper is organized as follows: section 2 presents the $\mathcal{L}_1$ adaptive control theory; in section 3 the control control systems architecture is described; section 4 introduces the helicopter equations used for simulations; in section 5 simulations results are presented; finally a section 6 of concluding marks ends this paper.

2. $\mathcal{L}_1$ ADAPTIVE CONTROL THEORY OVERVIEW

$\mathcal{L}_1$ adaptive control can be seen as an improvement to classical model reference adaptive control (MRAC) trough the introduction of a low pass filter in the control action. Such filter has the effect of decoupling the adaptation from the plant and therefore from robustness of the closed loop system. Due to the presence of the filter $\mathcal{L}_1$ adaptive control allows the usage of high adaptation rate without introducing unwanted or even dangerous oscillation in the plant. Figure 1 shows the general structure of output feedback $\mathcal{L}_1$ adaptive control. $A(s)$ is the plant model, $M(s)$ is the reference model, $C(s)$ is a low pass filter and $\hat{\sigma}$ is the disturbance estimates made trough the following adaptation law:

$$\dot{\hat{\sigma}}(s) = \Gamma \text{proj}(\hat{\sigma}, -\tilde{y}) \tag{1}$$

The reference model is the desired dynamics that the plant is desired to follow. The difference between the reference model output and the actual plant is used to estimate the uncertainty parameter value which includes both disturbances and model errors. The high values of Γ lead to fast adaptation but also to high derivatives and possibly oscillations in the control input u. The filter is then added to mitigate these effects and to decouple fast adaptation from robustness.

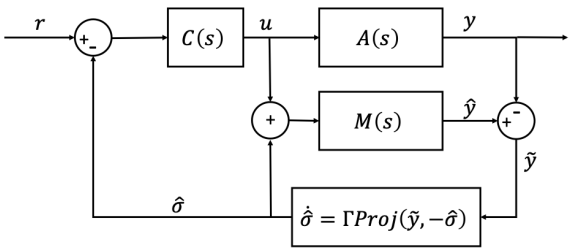

Figure 1: $\mathcal{L}_1$ adaptive control scheme

Filter and reference model are unitary gain stable systems having the following transfer functions:

$$C(s) = \frac{c}{s+c} \qquad M(s) = \frac{m}{s+m} \tag{2}$$

Assuming that Γ is sufficiently high the closed system response of the system in figure 1 is given by the following:

$$y(s) = H(s) C(s) r(s) - G(s) d(s) \tag{3}$$

Where $G(s)$ is defined as:

$$G(s) = H(s)(1 - C(s)) \tag{4}$$

and $H(s)$ is:

$$H(s) = \frac{A(s) M(s)}{C(s) A(s) + (1 - C(s)) M(s)} \tag{5}$$

From equation 3 it is possible to understand that disturbance rejection is achieved if the following condition holds:

$$\|G(s)\|_{\mathcal{L}_1} L < 1 \tag{6}$$

where is has been assumed that $d(t) = f(t, y(t))$ is lipschitz continuous and the following relations holds

$$| f(t, y_1) - f(t, y_2) | \leq L | y_1 - y_2 | \tag{7}$$

$$| f(t, y) | \leq L | y | + L_0 \tag{8}$$

$$L \geq 0, L_0 \geq 0 \tag{9}$$

The $d(t)$ function is not known but it is assumed that it is possible to choose a suitable conservative and high enough L constant in the $\mathcal{L}_1$ adaptive control design.

3. CONTROL SYSTEM ARCHITECTURE

In this paper, the helicopter control system is organized in two main control loops, as reported in figure 2. On one hand, the inner control loop on the attitude is based on PID controllers, as well as the heading hold and altitude hold controllers. On the other hand, $\mathcal{L}_1$ is

the controller for the external control loop on the speed. In this section a brief overview of the attitude control loop is given, then the entire $\mathcal{L}_1$ control system design for speed control is reported.

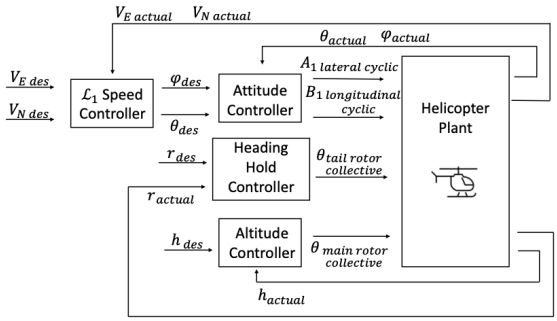

Figure 2: Helicopter control system architecture

3.1. PID attitude controllers

The inner control loop on helicopter attitude is based on PID technique on both the two distinct axes of roll and pitch. It consists of a cascade control system.[18] In the outer loop there is a primary controller with its dynamic that evaluates the set point for the inner loop. This should have a substantially faster dynamic than the outer loop in order to improve stability. As shown in figures 3, 4, the feedback signals are the roll rate p, the pitch rate q and roll and pitch angles ϕ and θ, respectively for the lateral and longitudinal axes.

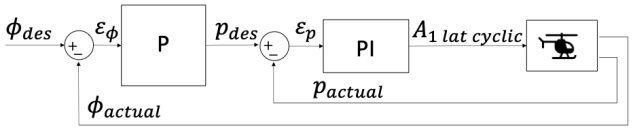

Figure 3: Roll controller architecture

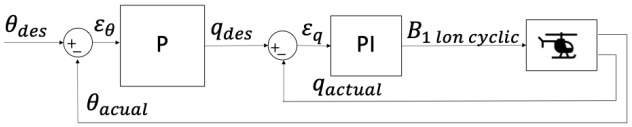

Figure 4: Pitch controller architecture

The inner loop deals with the angular rates p and q in a Proportional Integral scheme, while the outer loop concerns the angles ϕ and θ with a Proportional gain. The error signals are defined as follows, on roll axis:

$$\begin{cases} \epsilon_\phi = \phi_{des} - \phi \\ \epsilon_p = p_{des} - p \end{cases} \tag{10}$$

and on the pitch axis:

$$\begin{cases} \epsilon_\theta = \theta_{des} - \theta \\ \epsilon_q = q_{des} - q \end{cases} \tag{11}$$

The cascade P-PI control outputs result are the following:

$$\begin{cases} p_{des} = K_{P\phi}\epsilon_\phi \\ \delta_{lat} = K_{Pp}\epsilon_p + K_{Ip}\int_0^t \epsilon_p dt \end{cases} \tag{12}$$

$$\begin{cases} q_{des} = K_{P\theta}\epsilon_\theta \\ \delta_{lon} = K_{Pq}\epsilon_q + K_{Iq}\int_0^t \epsilon_q dt \end{cases} \tag{13}$$

where K_P are the proportional gains and K_I the integral gains.

3.2. PID heading hold and altitude hold controllers

Both heading hold and altitude hold controllers are based on PID control strategy, with a similar structure of that presented for the cascade attitude hold controller. In figure 5 the scheme of the heading hold controller is shown.

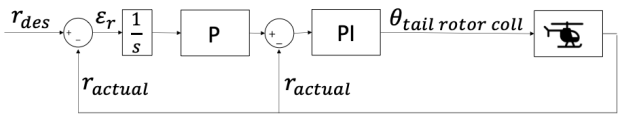

Figure 5: Heading hold controller architecture

There is a difference with the attitude hold controllers that lies in the input signal. As a matter of fact, the heading hold controller input signal is directly the yaw rate r instead of the yaw angle ψ. The desired yaw angle of the outer loop comes from the integration of the error signal on yaw rate ϵ_r. An appropriate initial value for the integration is set. The error signals are defined as follows:

$$\begin{cases} \epsilon_\psi = \int_0^t \epsilon_r dt \\ \epsilon_r = r_{des} - r \end{cases} \tag{14}$$

The cascade control output results to be:

$$\begin{cases} r_{des} = K_{P\psi}\epsilon_\psi \\ \delta_{coll\ tr} = K_{Pr}\epsilon_r + K_{Ir}\int_0^t \epsilon_r dt \end{cases} \tag{15}$$

Figure 6 shows the altitude hold control scheme.

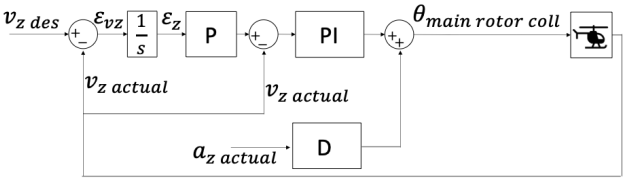

Figure 6: Altitude hold controller architecture

Vertical speed and acceleration acting on the main rotor collective are controlled. The pilot input is a reference vertical velocity, that is integrated to have a reference altitude similarly to the heading hold controller. The main difference with respect to the others PID presented controllers is in the presence of the derivative action on the vertical acceleration. The error signals are defined as:

$$\begin{cases} \epsilon_z = \int_0^t v_z dt \\ \epsilon_{v_z} = v_{zdes} - v_{zact} \end{cases} \tag{16}$$

The control output results to be:

$$\begin{cases} v_{zdes} = K_{Pz}\epsilon_z \\ \delta_{coll\ mr} = K_{Pv_z}\epsilon_{v_z} + K_{Iv_z}\int_0^t \epsilon_{\dot{z}} dt + K_{Da_z}a_z \end{cases} \tag{17}$$

3.3. $\mathcal{L}_1$ speed control design

Helicopter attitude is controlled trough a PI controller. The longitudinal and lateral dynamics used to design the $\mathcal{L}_1$ adaptive speed controller are those from reference roll and pitch attitude angles and actual lateral and longitudinal helicopter speed in vertical reference frame. The helicopter longitudinal and lateral states x_{lon} and x_{lat}, inputs u_{lon} and u_{lat} and outputs y_{lon} and y_{lat} are as follows:

$$\begin{aligned} &x_{lon} = (U, q, \theta)\,, &&x_{lat} = (V, p, \phi)\,, \\ &u_{lon} = \theta_{ref}, &&u_{lat} = \phi_{ref}, \\ &y_{lon} = \theta &&y_{lat} = \phi \end{aligned} \tag{18}$$

where U and V are longitudinal and lateral speed, θ and ϕ are pitch and roll attitude angles, q and p are pitch and roll rates, θ_{ref} and ϕ_{ref} are pitch and roll reference attitude angles. Longitudinal and lateral speed dynamics have been identified trough recursive least square algorithm during a flight simulation. The resulting identified matrices are, for longitudinal and lateral dynamics respectively, as follows:

$$A_{lon} = \begin{pmatrix} -0.0754 & 0.3836 & -9.6238 \\ 0.0299 & -15.4877 & -43.5876 \\ -0.0001 & 1.0014 & 0.0084 \end{pmatrix} \tag{19}$$

$$B_{lon} = \begin{pmatrix} -1.1820 \\ 35.7173 \\ -0.0149 \end{pmatrix} \tag{20}$$

$$A_{lat} = \begin{pmatrix} -0.0472 & 0.5084 & 9.6365 \\ 0.0001 & -0.2138 & -1.2305 \\ -0.0001 & 0.9966 & 0.0095 \end{pmatrix} \tag{21}$$

$$B_{lat} = \begin{pmatrix} -0.5275 \\ 0.7350 \\ 0.0015 \end{pmatrix} \tag{22}$$

Transfer functions for longitudinal and lateral speed dynamics are as follows:

$$U(s) = A_{lon}(s)\,\theta_{ref}(s) \tag{23}$$

$$A(s)_{lon} = \frac{-1.182\left(s^2 + 3.767s + 332.8\right)}{(s+11.79)(s+3.681)(s+0.08191)} \tag{24}$$

$$V(s) = A_{lat}(s)\,\phi_{ref}(s) \tag{25}$$

$$A(s)_{lat} = \frac{-0.52752(s-3.762)(s+3.231)}{(s+0.04682)(s^2+0.2047s+1.225)} \tag{26}$$

Such system dynamics are used to design the $\mathcal{L}_1$ adaptive speed controller by checking that the condition 6 is satisfied in order to achieve closed loop robustness.

Chosen reference dynamics that lead the closed loop plant to achieve desired dynamics performances are the following:

$$M(s)_{lon} = \frac{0.5}{s+0.5} \tag{27}$$

$$M(s)_{lat} = \frac{0.45}{s+0.45} \tag{28}$$

Low pass filters that satisfies condition 6 are:

$$C(s)_{lon} = \frac{7}{s+7} \tag{29}$$

$$C(s)_{lat} = \frac{10}{s+10} \tag{30}$$

In this design the longitudinal and lateral speed controllers are separated and couplings are not considered. The $\mathcal{L}_1$ adaptive controller is able to compensate for couplings due to its fast adaptation properties, indeed if a certain speed is demanded to the helicopter on one of the axis the coupling on the other one can be seen as a disturbance and then the $\mathcal{L}_1$ is able to handle it.

4. HELICOPTER MODEL

This section summarizes the dynamical model of the small-scale helicopter used for simulations, whose data are reported in Appendix 6.

A conventional single main rotor with one tail rotor helicopter is considered. Each helicopter component, i.e. main rotor, tail rotor and fuselage, have been modelled and the resultant forces and moments applied in the center of gravity are the sum of the contributions of all the helicopter components plus the gravitational forces. The Earth is considered flat and non-rotating with a uniform gravity field. The helicopter mass and its distribution are constant.

Three right–handed orthogonal reference frames are considered. Let $\mathbb{F}_E = \{O; \mathbf{x}_E, \mathbf{y}_E, \mathbf{z}_E\}$ be the North-East-Down (NED) frame; $\mathbb{F}_{hw} = \{H; \mathbf{x}_{hw}, \mathbf{y}_{hw}, \mathbf{z}_{hw}\}$ be the Hub-Wind frame, whose origin is in the helicopter hub; $\mathbb{F}_{hb} = \{H; \mathbf{x}_{hb}, \mathbf{y}_{hb}, \mathbf{z}_{hb}\}$ the Hub-Body frame, that coincides with the Hub-Wind when the system sideslip is zero, and $\mathbb{F}_b = \{P; \mathbf{x}_b, \mathbf{y}_b, \mathbf{z}_b\}$ the Body frame, located at the helicopter center of gravity, according to those presented in[19][20] .

Helicopter dynamics is described by Newton-Euler equations of motion projected in the body system $\mathbb{F}_B$:

$$\dot{\mathbf{v}} = -\boldsymbol{\omega} \times \mathbf{v} + \mathbf{F}^{\mathbf{e}}/\mathbf{m} \tag{31}$$

$$\dot{\boldsymbol{\omega}} = \boldsymbol{J}^{-1}\left[-\boldsymbol{\omega} \times (\boldsymbol{J}\,\boldsymbol{\omega}) + \mathbf{M}^{\mathbf{e}}\right] \tag{32}$$

where $\boldsymbol{\omega}$ is the angular velocity, $\mathbf{v}$ is the linear body velocity, $\mathbf{F}^{\mathbf{e}}$ and $\mathbf{M}^{\mathbf{e}}$ are the external forces and moments vectors, $\boldsymbol{J}$ is the inertia tensor about CG with respect to $\mathcal{F}_B$, and m is the total mass of the rotorcraft. The external force acting on the rotorcraft is made of gravity, $\boldsymbol{F}^{(g)}$, and aerodynamic, $\boldsymbol{F}^{(a)}$, contributions. The gravity force vector is expressed as:

$$\boldsymbol{F}^{(g)} = \Pi_{be}\begin{bmatrix}0\\0\\m\,g\end{bmatrix} = m\,g\begin{bmatrix}-\sin\theta\\ \sin\phi\,\cos\theta\\ \cos\phi\,\cos\theta\end{bmatrix} \tag{33}$$

where g is the gravitational acceleration.

The characterization of the aerodynamic forces, $\boldsymbol{F}^{(a)} = [X,\, Y,\, Z]^T$, and moments, $\boldsymbol{M}^{(a)} = [L,\, M,\, N]^T$, is performed on the basis of the model detailed in.[19] Contributions are provided by helicopter main rotor, tail rotor and fuselage. Air parameters are calculated from the International Standard Atmosphere (ISA) model as a function of rotorcraft altitude.[21]

4.1. Main rotor model

The following assumptions are made for the main rotor model: a) rotor blades are rigid in bending and torsion; b) flapping angles are small and the simple strip theory[22] is followed; c) blade flow stall is not considered; d) main rotor blade flapping is approximated by the first harmonic terms with time-varying coefficients, that is

$$\beta(t) = a_0 - a_1\,\cos\xi - b_1\,\sin\xi \tag{34}$$

where a_0 is a preset constant and ξ is blade azimuth. Coefficients $a_1(t)$ and $b_1(t)$ respectively represent the longitudinal and the lateral tilt of the rotor tip-path plane.

Given the above assumptions, momentum theory is utilized and blade forces are analytically integrated over the radius. Detailed expressions for the derivation of forces and moments are given in Ref.[19] Concerning the inflow modelling, the Pitt-Peters dynamic inflow model[23] has been used, only considering a uniform inflow.

4.2. Tail rotor model and fuselage

The tail rotor is modeled according as in Ref.[19] without cyclic pitch. Provided that the flapping frequency is typically much higher than that of the main rotor system, the tail rotor tip-path plane dynamics is not considered. Forces and moments and flapping angles are steady state solutions.

The fuselage is represented as a virtual flat plate drag source having three dimensions.[24] Forces and moments are evaluated as functions of the angle of attack and of the sideslip angle.

5. SIMULATION RESULTS

This section presents the main results of the simulation campaign performed to test the quality of the controller architecture in terms of performance and robustness. The nonlinear model described in Section 4, characterized by the helicopter data listed in Appendix A, has been utilized for the simulations. It has been implemented in a Matlab/Simulink® environment, where differential equations are solved by Dormand–Prince ode8 method with a frequency of 1000 Hz.[25] The following steps have been carried out: 1) the trim conditions are determined for different cruise speeds, 2) a linearization procedure is then applied to the complete model about the equilibrium points, and 3) an open–loop dynamic analysis is performed to investigate the helicopter control and stability properties. In what follows, the behaviour of the $\mathcal{L}_1$ speed controller is shown in Section 5.1 in case of multistep inputs and in Section 5.2 in case of pilot inputs. For this second instance, the inputs are given to the simulator through the use of a Joystick Logitech Saitek X52 Pro interfaced with Simulink®.

5.1. Multistep signal response

In this test the helicopter is asked to follow a multistep reference speed on longitudinal or lateral axes. The $\mathcal{L}_1$ adaptive control proves to be able to track the reference model $M(s)$ response on both axis allowing the helicopter to achieve the desired performances. Speed profiles are showed in figures 7 and 8.

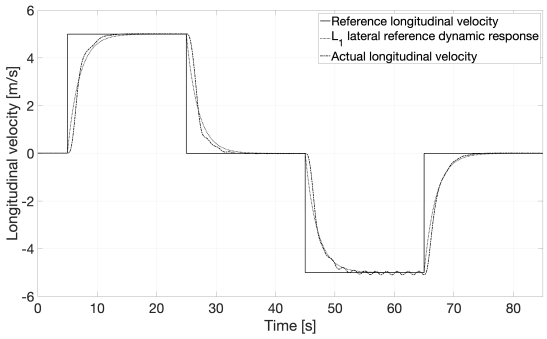

Figure 7: Longitudinal response to longitudinal speed step commands

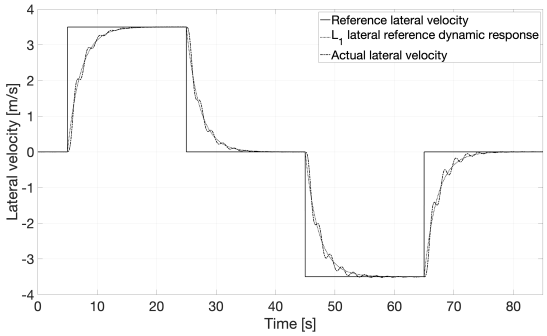

Figure 8: Lateral response to lateral speed step commands

The $\mathcal{L}_1$ adaptive speed control was assumed to be able to reject coupling disturbances due to its fast adaptive rates. Figures 9 and 10 show the coupling effects on lateral and longitudinal axis respectively when the multistep reference is given on the longitudinal or on the lateral axis. Couplings are present, but their magnitude is small, compared to demanded speed, and these decrease in time.

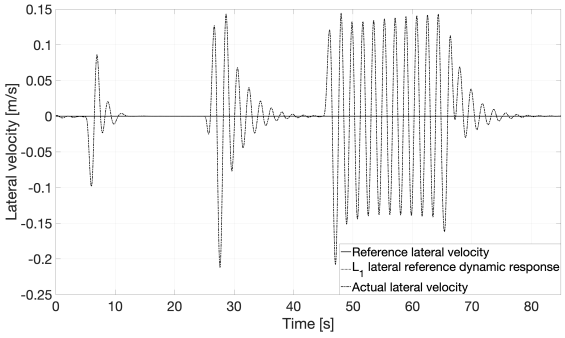

Figure 9: Lateral response to longitudinal speed step commands

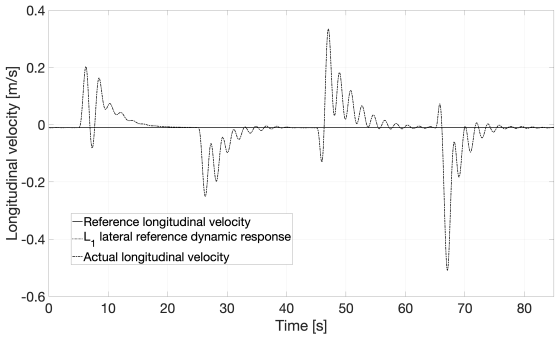

Figure 10: Longitudinal response to lateral speed step commands

5.2. Pilot input in simulation

The helicopter is then asked to follow a pilot generated speed reference. In figures 11 and 12 longitudinal and lateral speed are displayed. The controller proves to be able to track the reference with the desired dynamics.

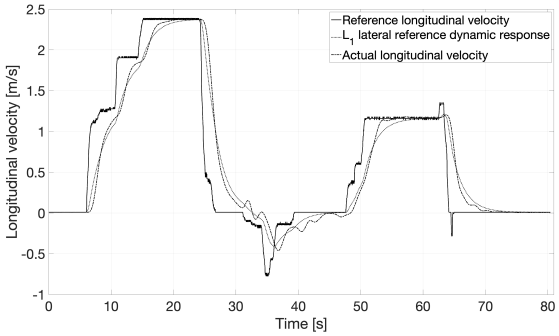

Figure 11: Longitudinal response to pilot commands

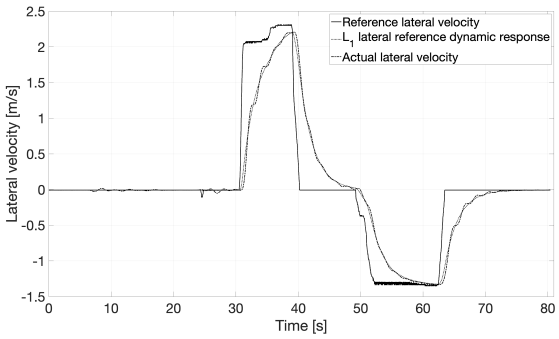

Figure 12: Lateral response to pilot commands

The same pilots commands are then given to the helicopter in presence of wind disturbances. Three kind of mathematical models are used to simulate the wind. The first type of disturbance is a discrete gust on the three axes with an amplitude of $[u_g v_g w_g] = [3.5\ 3.5\ 3.0]$ m/s, where u_g, v_g and w_g are the gust components. The second disturbance is a discrete Dryden wind turbulence model. It is based on the Dryden spectral representation.[26] In this case, the wind speed is set to 15 m/s at 6 m of altitude with a direction of 0 degrees clockwise from north. The third wind model is the shear one, that is based on what is reported in the Military Specification MIL-F-8785C.[27] The wind speed is set as in the case of Dryden turbulence. Figures 13 and 14 show the wind speed profile along longitudinal and lateral axes. In a real flight condition the pilot would change the command inputs in order to compensate for the wind disturbances. Giving the helicopter the same command inputs as in the cases when the wind disturbance is not present allows to test the rejection capabilities of the $\mathcal{L}_1$ adaptive controller alone. It is like the pilot ignores the disturbances and leaves the controller the task of fully compensate for the disturbance. Figures 15 and 16 show the test result proving that the controller itself is capable of rejecting the speed disturbances induced by wind.

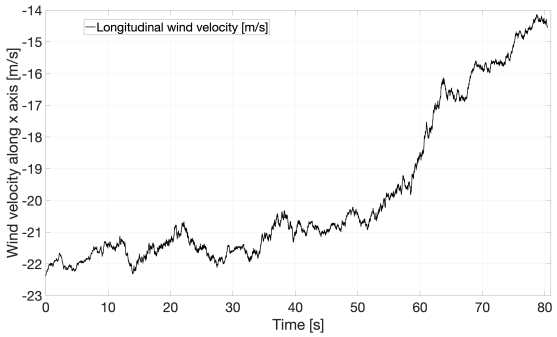

Figure 13: Wind speed profile along longitudinal axis

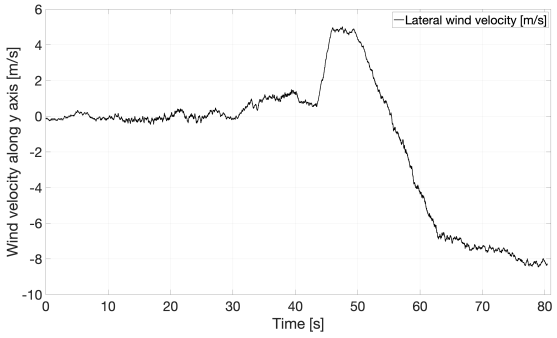

Figure 14: Wind speed profile along lateral axis

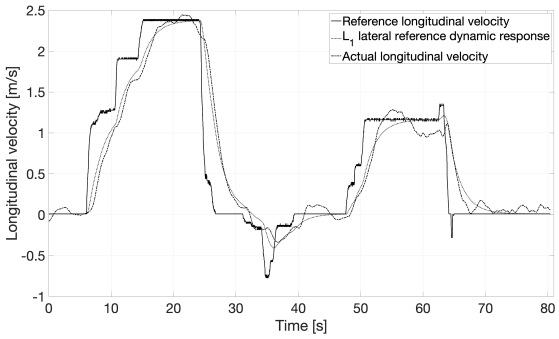

Figure 15: Longitudinal response to pilot commands in presence of wind

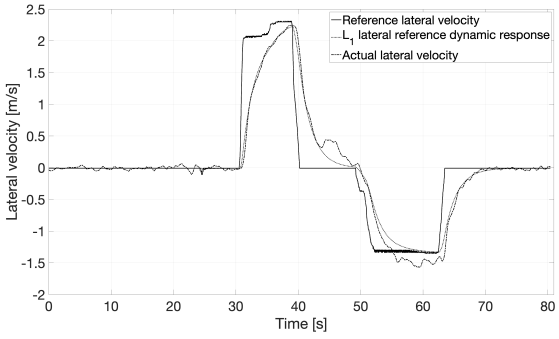

Figure 16: Lateral response to pilot commands in presence of wind

Finally figures 17 and 18 shows the adaptation terms σ_{lat} and σ_{lon} both in absence and in presence of wind for piloted flight. On the longitudinal axis the helicopter faces a wind speed that varies almost from 22 m/s to 14 m/s, as reported in figure 13. The σ_{lon} adaptation term indeed is almost only shifted by a constant value. On the lateral axis the helicopter faces an abrupt gust slightly after $40s$, as showed in figure 14, that justifies the high σ_{lat} change after this time instant in the plot of figure 18.

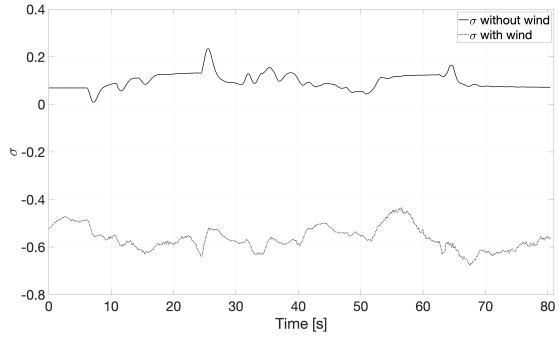

Figure 17: Longitudinal adaptive estimation

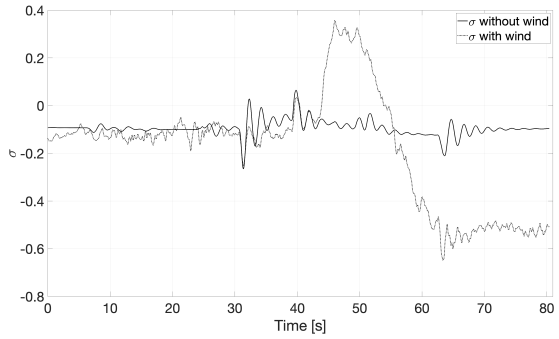

Figure 18: Lateral adaptive estimation

6. CONCLUSIONS

In the present paper, the $\mathcal{L}_1$ adaptive control theory has been used to design a speed hold control loop for a helicopter. The $\mathcal{L}_1$ adaptive control strategy used is output feedback and the adaptive law is Lyapunov based. The controller has been tested by means of a simulation test campaign. Results proved that the designed controller is able to follow the desired reference dynamics and to reject disturbances. In fact, wind disturbances have been added in the simulation environment to test the control system robustness. Pilot workload reduction has also been proved trough the comparison of speed reference tracking both in absence and in presence of wind disturbances. The same pilot commands are given to the system as inputs in both cases. Results show that the system is capable to track the reference even in the situation in which the pilot does not compensate for the disturbances, as it would happen in a real flight. This result is justified by the fact that the adaptive speed controller compensates for external disturbances instead of the pilot. In future, the performances of the $\mathcal{L}_1$ adaptive speed control system may be tested experimentally through an extensive flight test campaign.

COPYRIGHT STATEMENT

ACKNOWLEDGEMENTS

APPENDIX A

Table 1: Helicopter relevant parameters.

Parameter	Symbol	Value	Units
Vehicle data			
Mass	m	4.8	kg
Center of gravity stationline	STA_{CG}	0.34	m
Center of gravity buttline	BL_H	0	m
Center of gravity waterline	WL_H	0.174	m
Moment of inertia	$I_x,\ I_y,\ I_z$	0.0465, 0.2971, 0.2567	kg m^2
Inertia products	$I_{xy},\ I_{yz},\ I_{xz}$	0.0079, 0.0033, 0.0006	kg m^2
Main Rotor			
Number of blades	N_b	2	-
Radius	R_{MR}	0.79	m
Chord	c_{MR}	0.06	m
Rotational speed	Ω_{MR}	1995.3	rpm
Hinge offset	ε	0.0314	m
Flapping spring constant	K_β	162.69	N m/rad
Tangent of δ_3	K_1	0	-
Blade twist	θ_{tMR}	0	rad
Precone angle	a_{0MR}	0	rad
Solidity	σ_{MR}	0.0479	-
Lift curve slope	a_{TR}	2*π	1/rad
Blade inertia moment	I_β	0.0344	kg m^2
MR hub stationline	STA_H	0.3305	m
MR hub buttline	BL_H	0	m
MR hub waterline	WL_H	0.35	m
Tail Rotor			
Number of blades	N_b	2	-
Radius	R_{TR}	0.115	m
Chord	c_{TR}	0.031	m
Rotational speed	Ω_{TR}	9976	rpm
Tangent of δ_3	K_{1TR}	0	-
Blade twist	θ_{tMR}	0	rad
Solidity	σ_{TR}	0.1716	-
Lift curve slope	a_{TR}	2*π	1/rad
Blade inertia moment	I_β	0.00002665	kg m^2
TR hub stationline	STA_{TR}	1.385	m
TR hub buttline	BL_{TR}	0.052	m
TR hub waterline	WL_{TR}	0.205	m
Fuselage (Fus.)			
Fus. aerodynamic ref. point stationline	STA_{FUS}	0	m
Fus. aerodynamic ref. point buttline	BL_{FUS}	0	m
Fus. aerodynamic ref. point waterline	WL_{FUS}	0	m
Frontal area	S_{front}	0.02042	m^2
Lateral area	S_{lat}	0.0633	m^2
Top area	S_{top}	0.09739	m^2

References

[1] Muchiri, G. N., and S. Kimathi., A review of applications and potential applications of UAV. - Proceedings of the Sustainable Research and Innovation Conference. 2022. p. 280-283.

[2] de Angelis, E.L., Giulietti, F., Dynamic stability and control of rotorcraft for suspended load transportation: an analytical approach. - European Rotorcraft Forum 2022, Winterthur, paper No.94, 2022.

[3] Kumar, V., Michael, N., Opportunities and challenges with autonomous micro aerial vehicles. - The International journal of robotics research, vol. 31, no. 11, pp. 1279–1291, 2012. https://doi.org/10.1177/0278364912455954

[4] Raptis, I.A. and Valavanis, K. P., Linear and Nonlinear control of small-scale unmanned helicopters. - 2011. Intelligent systems 45. doi:10.1007/978-94-007-0023-9.

[5] Hu, J., Gu, H., Survey on flight control technology for large-scale helicopter. - International journal of aerospace engineering, vol. 17, Article ID 5309403, 14 pages, 2017. https://doi.org/10.1155/2017/5309403

[6] Anavatti S. G., Santoso F., Garratt M. A., Progress in adaptive control systems: past, present, and future. - 2015 International Conference on Advanced Mechatronics, Intelligent Manufacture, and Industrial Automation (ICAMIMIA), pp. 1-8, 2015. DOI: 10.1109/ICAMIMIA.2015.7537196

[7] Hovakimyan N., Cao, C., L1 Adaptive Control Theory: Guaranteed Robustness with Fast Adaptation. - IEEE Control Systems Magazine, vol. 31, no. 5, pp. 112-114, Oct. 2011. doi:10.1109/MCS.2011.941837.

[8] Cao, C., Hovakimyan, N., Design and Analysis of a Novel L1 Adaptive Controller, Part I: Control Signal and Asymptotic Stability. - 2006 American Control Conference, 2006, pp. 3397-3402. doi: 10.1109/ACC.2006.1657243.

[9] Cao, C., Hovakimyan, N., Design and Analysis of a Novel L1 Adaptive Controller, Part II: Guaranteed Transient Performance. - 2006 American Control Conference, 2006, pp. 3403-3408. doi: 10.1109/ACC.2006.1657244.

[10] Cao, C., Hovakimyan, N., L1 Adaptive Output Feedback Controller to Systems of Unknown Dimension. - 2007 American Control Conference, 2007, pp. 1191-1196. doi:10.1109/ACC.2007.4282999.

[11] Gregory, I., Cao, C., Xargay, E., Hovakimyan, N. and Zou, X., L1 adaptive control design for NASA AirSTAR flight test vehicle - AIAA Guidance, Navigation, and Control Conference, Chicago, IL., 2009. doi: 10.2514/6.2009-5738

[12] Wang, J., Vijay, V. P., Cao, C., Hovakimyan, N., Lavretsky, E., Novel L1 adaptive control methodology for aerial refueling with guaranteed transient performance. - Journal of Guidance Control and Dynamics, Vol. 31, 2008, 182–193. doi:10.2514/1.31199

[13] Hellmundt, F., Wildschek, A., Maier, R., Osterhuber, R., Holzapfel, F., Comparison of L1 Adaptive Augmentation Strategies for a Differential PI Baseline Controller on a Longitudinal F16 Aircraft Model. - Advances in Aerospace Guidance, Navigation and Control, 99–118, 2018. doi:10.1007/978-3-319-17518-8-7

[14] Bichlmeier, M., Holzapfel, F., Xargay, E., Hovakimyan, N., L1 adaptive augmentation of a helicopter baseline controller. - AIAA Guidance, Navigation, and Control (GNC) Conference, 2013. doi:10.2514/6.2013-4855

[15] Song, T., Wang, J., Lin, D., Pei, P. L1 adaptive control design of a helicopter in vertical flight. - Proceedings of the Institution of Mechanical Engineers, Part G: Journal of Aerospace Engineering, Vol. 234, No. 14, 2014, 2089–2099, 2020. doi: 10.1177/0954410020926619

[16] Guerreiro, B. J., Silvestre, C., Cunha, R., Cao, C., Hovakimyan, N., L1 adaptive control for autonomous rotorcraft. - American Control Conference, 3250–3255, 2009. doi:10.1109/ACC.2009.5159940

[17] Bertolani, G., Ryals, A.D., Giulietti, F., Pollini, L., Adaptive attitude control of an unmanned helicopter. - Ceas Aerospace Europe Conference, Warsaw, November, 2021.

[18] Szafranski, G., Roman, C., Different approaches of PID control UAV type quadrotor. - The international micro air vehicles conference, 70–75, 2011.

[19] Talbot, P. D., Tinling, B. E., Decker, W. A., Chen, R. T. N., A mathematical model for a single main rotor helicopter for piloted simulation. - Ames Reasearch Center, Mffett, Field, California, 1982.

[20] de Angelis, E.L., Giulietti, F., Rossetti, G., Turci, M., Albertazzi, C., Toward smart air mobility:control system design and experimental validation for an unmanned light helicopter. - European Rotorcraft Forum 2022, Winterthur, paper No.92, 2022.

[21] U.S. Government Printing Office, U.S. Standard Atmosphere, NOAA-S/T 76-1562, Washington, D.C., 1976, 1–241.

[22] J.G. Leishman, Principles of Helicopter Aerodynamics, 2nd Edition, Cambridge University Press, New York, 2006, Chs. 2 and 5.

[23] Peters, D. A.,HaQuang, N., Dynamic inflow for practical applications. - Journal of the American Helicopter Society, Vol. 33, No. 4, 1988.

[24] Heffley, R. K., Mnich, M. A., Minimum-complexity helicopter simulation math model. - Ames Reasearch Center, Mffett, Field, California, 1988.

[25] Dormand, J.R., Prince, P.J., A family of embedded Runge-Kutta formulae. - Journal of Computational and Applied Mathematics, Vol. 6, Issue 1,pp 19–26, 1980. https://doi.org/10.1016/0771-050X(80)90013-3.

[26] U.S. Military Specification MIL-F-8785C, November 5, 1980.

[27] U.S. military handbook MIL-HDBK-1797B, April 9, 2012.